

Solar PV Fed Induction Motor Driven Water Pumping System Using High Gain Converter

Reshma Raj O¹, Biji G²

¹PG Scholar, Dept. of EEE, Govt. Engineering College Barton Hill, Kerala, India

²Assistant Professor, Dept. of EEE, Govt. Engineering College Barton Hill, Kerala, India

Abstract - In this paper, a solar water pumping system using an induction motor drive (IMD) is presented. This solar PV water pumping system consists of mainly two stages of power conversion. In first stage, by controlling the duty ratio of the DC-DC boost converter it extracts maximum power from solar PV array. By controlling the motor speed, the DC bus voltage is maintained constant. Here a high gain converter is used. By reducing the number of solar modules the output voltage of PV can be reduced. To control the duty ratio, a perturb and observe (P and O) based maximum power point tracking (MPPT) control technique is utilized. For operating the induction motor drive, a scalar controlled voltage source inverter is used. By the proposed control scheme the stator frequency reference of induction motor drive is obtained. The proposed system is modelled and its performance is simulated in detail. The performance under different operating conditions are obtained using MATLAB/Simulink software.

Key Words : MPPT, Photovoltaic (PV), water pumping, scalar control, induction motor drive (IMD)

1. INTRODUCTION

The solar PV generation is used in many applications. One of the application is in solar water pumps. Water pumping systems based on photovoltaic technology are better for rural areas where connection to the grid can be difficult and expensive. The standalone solar water pumping system uses two control mechanisms to make the DC link voltage constant at varying irradiances [1]. The solar water pumps [2] and [3] are becoming popular in rural areas, where the electricity is not available. These water pumps are used in remote areas for water treatment plant, irrigation and agriculture purpose. In India, many people depends on agriculture. So irrigation is necessary for good production. Compared to diesel based water pumping systems the solar PV based water pumping systems [4] are more convenient in terms of cost and pollution.

In comparison with other commercial motors, induction motor drive has good performance. This helps to develop maintenance free and cheap water pumping system [5]. The water pumping system requires MPPT algorithm to operate under different irradiation levels. A comparative

study on different MPPT techniques are given in [6]-[8]. From this, the INC technique requires more computational steps. In comparison with the solar PV grid interfaced systems [9], the main challenge in water pumping system is the control of active power. A V/f control method is used to control the induction motor drive given in [10]-[12]. This V/f method is very simple and easy to implement. The water pumping system with a DC-DC converter and VSI is used for water pumping application in [13]-[15]. But this causes instability in DC link voltage. The DC-DC boost converter given in [16] and [17] has high gain. But the drawback is that the number of components used are more and its cost is high. The parameters of the induction motor drive can be obtained from [18]. The direct torque control and vector control methods are very complex and it requires many current sensors for its implementation [19]. The areas which have the electricity availability, may utilize the grid interfaced solar PV water pumps [20].

In this paper, the proposed work deals with a three-phase induction motor drive for solar water pumping, which meets the requirement of life without electricity in remote locations. The varying nature of solar PV generation affects the water pumping system. So to overcome this problem, here 2 control mechanisms are used. They are MPPT control and V/f control. The water pumping system powered directly from PV array, requires MPPT algorithms to operate under different irradiation levels and to extract the peak power from a solar PV array. Here a P and O (Perturb and Observe) based technique is used to obtain the peak power from the solar PV array. So that it can reduce the computational steps. Therefore, the proposed PV fed water pumping system produces peak voltage even at low radiation. When the solar radiation reduces the system can maintain a constant DC link voltage. The existing system [1] uses a low gain converter and an INC method of MPPT control for tracking maximum power from PV array. The drawback of existing system is that it uses a low gain converter so that it requires more number of solar modules and the THD of the system is high.

2. PROPOSED SYSTEM

The system configuration for PV water pumping system is shown in Fig -2 and its block diagram is shown in Fig -1.

It consists of a PV array followed by a modified quadratic boost converter. A VSI is used to provide pulse width modulated voltage input to the motor and pump assembly. The power from a PV array is regulated using a perturb and observe (P and O) method to attain its maximum value with available radiation. The V/f control is used to give reference speed to IMD.

The working of the system is when sunlight falls on PV array the voltage across the array is V_{PV} . It will be in varying nature. So it is given to a proposed boost converter so that it can increase the gain of the system. Here the voltage and current from PV array are given to the MPPT and by P and O method duty ratio is obtained. Then gate pulse is given to the switch. The capacitor C_f is used to filter input current ripples. Here when the switch is in ON condition, the current flows through inductor L_1 and it is get charged and then current flows through diode D_1 . So diode D_1 is forward biased and current flows through the switch. The capacitor C_1 is discharging at that time so the inductor L_2 is get charged by that and then current flows through the switch. The capacitor C_{DC} will be discharging at that time. Here diode D_3 and diode D_2 will be in reverse biased condition. When switch is in OFF condition, inductor L_1 and L_2 will be discharging. The capacitor C_1 is charged by inductor L_1 and C_{dc} will be charged by inductor L_2 . Here diode D_1 is reverse biased and diodes D_2 and D_3 are forward biased.

The voltage across DC bus is compared with the reference DC voltage and an error is obtained. It is given to a PI controller. The PI controller makes the error to zero. The output of PI controller is speed. It is then converted to reference frequency. The frequency is given to V/f control and its output is given to SPWM generator. It generates the switching pulses for each switches in the inverter and is given to induction motor and pump. The advantage of the system is at varying radiations, the DC bus voltage is maintained at constant by the action of PI controller.

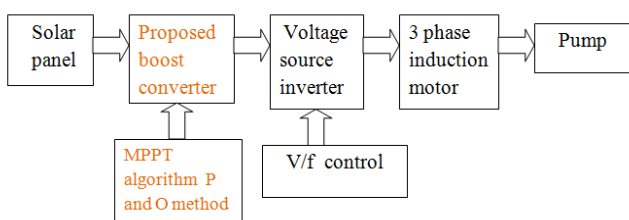


Fig -1: Block diagram of the proposed system

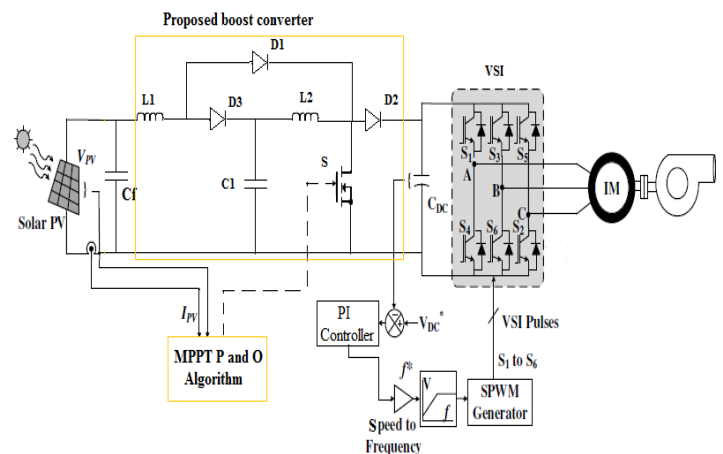


Fig -2: Proposed solar water pumping system

2.1. Design of solar PV array

An induction motor of 373W (0.5HP) is selected for the proposed system. If losses of the pump and motor are neglected, the capacity of the PV array should be equivalent to the motor capacity. In this case, the PV array is selected as of 500W.

$$P_{mp} = (N_p \times I_{mp}) \times (N_s \times V_{mp}) = 500W \quad (1)$$

where, P_{mp} is the maximum power that can be drawn from panels at a given radiation, V_{mp} is the PV panel voltage at MPP and I_{mp} is the current at MPP. N_s and N_p are the number of modules connected in series and parallel, respectively. Considering an open circuit voltage of the panel to be near to a DC link voltage and power drawn from a panel to be 500W, number of modules in series and parallel are selected to be 3 and 1. The individual module and array specifications are provided in Table -1.

Table -1: Specifications of solar module and array

Specifications	Values
Module peak power of the single module	169.5W
Module open circuit voltage (V_{oc})	41.79V
Module short circuit current (i_{sc})	6.25A
Module voltage at MPP (V_{mp})	33.9V
Module current at MPP (i_{mp})	5A
Array peak power (P_{mp})	500W
Array open circuit voltage (V_{oc})	125.37V
Array short circuit current (I_{sc})	6.25A
Array voltage at MPP (V_{mp})	100V
Array current at MPP (I_{mp})	5A

2.2. Selection of DC link voltage

The DC bus voltage of VSI is estimated from a relation as,

$$m \times \frac{V_{DC}}{2\sqrt{2}} = \frac{V_{L-L}}{\sqrt{3}} \quad (2)$$

where, m is the modulation index and V_{L-L} is a line voltage across the motor terminals. Hence,

$$V_{DC} = \frac{2\sqrt{2}}{\sqrt{3}} \times 400 = 653V \quad (3)$$

the voltage which is required when modulation index is 1. The DC link voltage is chosen to be 653 V.

2.3. Design of proposed boost converter

In this proposed boost converter, it is formed by connecting the conventional boost converter with another boost converter back to back using a single switch. Thus it forms a quadratic boost converter.

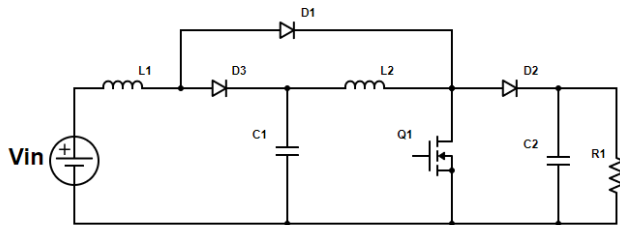


Fig -3: Circuit diagram of proposed boost converter

The voltage gain of the quadratic boost converter is more than the conventional boost converter. So by connecting this converter to the proposed system its voltage gain can be improved. It consists of 2 modes of operation.

In mode 1, when switch is turned ON, the current flows through inductor L_1 and then to diode D_1 . So diode D_1 is forward biased then current flows through the switch. The capacitor C_1 discharges and inductor L_1 gets charged and then current flows through the switch. So diode D_3 is in reverse biased condition. The capacitor C_2 that is equal to C_{dc} in the proposed system discharges and so the diode D_2 is in reverse biased condition.

$$V_{in} - V_{L1} = 0 \quad (4)$$

$$V_{L1} = V_{in} \quad (5)$$

$$V_{C1} - V_{L2} = 0 \quad (6)$$

$$V_{L2} = V_{C1} \quad (7)$$

In mode 2, when switch is turned OFF, then inductor L_1 gets discharged and current flows through diode D_3 . The diode D_3 is forward biased. The capacitor C_1 is charged by inductor L_1 . The inductor L_1 get discharged and current flows through diode D_2 . Then current flows through capacitor C_2 and it is get charged by inductor L_2 and then current flows through the load.

$$V_{in} - V_{C1} = V_{L1} \quad (8)$$

$$V_{C1} - V_{L2} - V_{C2} = 0 \quad (9)$$

$$V_{L2} = V_{C1} - V_{C2} = V_{C1} - V_{C0} \quad (10)$$

When switch is on,

$$\frac{\Delta i_{L1}}{DT_s} = \frac{V_{in}}{L_1} \quad (11)$$

$$(\Delta i_{L1})_{ON} = \frac{V_{in}DT_s}{L_1} \quad (12)$$

$$\frac{\Delta i_{L2}}{DT_s} = \frac{V_{C1}}{L_2} \quad (13)$$

$$(\Delta i_{L2})_{ON} = \frac{V_{C1}DT_s}{L_2} \quad (14)$$

When switch is off,

$$\frac{\Delta i_{L1}}{(1-D)T_s} = \frac{(V_{in}-V_{C1})}{L_1} \quad (15)$$

$$(\Delta i_{L1})_{OFF} = \frac{(V_{in} - V_{C1})(1 - D)T_s}{L_1} \quad (16)$$

$$\frac{\Delta i_{L2}}{(1-D)T_s} = \frac{(V_{C1}-V_0)}{L_2} \quad (17)$$

$$(\Delta i_{L2})_{OFF} = \frac{(V_{C1} - V_0)(1 - D)T_s}{L_2} \quad (18)$$

Combining eqn 12 and 16,

$$(\Delta i_{L1})_{ON} + (\Delta i_{L1})_{OFF} = 0 \quad (19)$$

$$\frac{V_{in}DT_s}{L_1} + \frac{(V_{in} - V_{C1})(1 - D)T_s}{L_1} = 0 \quad (20)$$

$$V_{in} = (1-D) V_{C1} \quad (21)$$

Combining eqn 14 and 18,

$$(\Delta i_{L2})_{ON} + (\Delta i_{L2})_{OFF} = 0 \quad (22)$$

$$\frac{V_{C1}DT_s}{L_2} + \frac{(V_{C1} - V_0)(1 - D)T_s}{L_2} = 0 \quad (23)$$

$$V_{C1} = (1-D) V_0 \quad (24)$$

Sub eqn 24 in 21,

$$V_{in} = (1 - D)^2 V_0 \quad (25)$$

$$\frac{V_o}{V_{in}} = \frac{1}{(1-D)^2} \quad (26)$$

2.4. Design of pump

For a 0.5 hp (373W), 400V, 50Hz, 4 pole, 1425 rpm 3 phase induction motor.

$$P_o = 746 \times 0.5 = 373W \quad (27)$$

$$T = \frac{P}{\omega} \quad (28)$$

$$\omega = \frac{2\pi N}{60} = \frac{2\pi 1425}{60} = 149.22 \text{ rad/s} \quad (29)$$

$$T = \frac{P}{149.22} = 2.49Nm \quad (30)$$

For a selected water pump, proportionality constant (K_{pump}) is given as,

$$K_{pump} = \frac{T_L}{\omega^2} \quad (31)$$

$$K_{pump} = \frac{T_L}{\omega^2} = \frac{2.49}{149.22^2} = 1.12 \times 10^{-4} \quad (32)$$

where, T_L is the load torque of water pump, which is equal to the torque offered by an induction motor under steady state operation and ω is the rotational speed of the rotor in rad/sec.

3. CONTROL SCHEME FOR PROPOSED SYSTEM

The proposed topology is a two stage power conversion system for a solar PV array fed water pumping. It uses scalar control for IMD operation and perturb and observe (P and O) method for maximum power extraction from the PV array. The simplicity and ease of implementation of scalar control overshadows precise but computation intensive control algorithms such as direct torque control and vector control. The voltage and current of PV array are sensed and fed to the P and O algorithm. Based on the change in voltage, current and power, this algorithm decides the duty ratio of the proposed boost converter. The proposed boost converter output voltage is maintained to a constant value using a proportional-integral (PI) controller. In the existing system[1] the voltage and current of PV array are sensed and fed to INC algorithm. Here the drawback is that it has more computational complexity. The V/f control generates the switching logic for VSI using sinusoidal pulse width modulation. If DC link voltage is higher than the reference value, the PI controller increases the reference speed given to V/f control and vice versa. The sum of two quantities gives a resultant speed reference f^* for IMD, which is fed to V/f control algorithm. The DC link voltage error is estimated as,

$$V_{DCr} = V_{DC}^* - V_{DC} \quad (33)$$

The output of the DC link voltage PI controller is ω_{DCr} . The reference frequency of the IMD is as,

$$f^* = \frac{1}{2\pi} \omega_{DCr} \quad (34)$$

3.1. Perturb and Observe method for MPPT

The perturb and observe (P and O) algorithm is generally the most commonly applied in the control of MPPT algorithm for the PV array. It has simple structure, easy to implement, low cost, reduced number of parameters, the possibility to introduce improvements and may result in high-level efficiency. This algorithm is depending on finding the relation between PV module output power and its voltage. In this technique, a small perturbation is introduced to cause the power variation of the PV module. The PV output power is periodically measured and compared with the previous power. If the output power increases, the same process is continued otherwise perturbation is reversed. In this algorithm perturbation is provided to the PV module or the array voltage. The PV module voltage is increased or decreased to check whether the power is increased or decreased. When an increase in voltage leads to an increase in power, this means the operating point of the PV module is on the left of the MPP. Hence further perturbation is required towards the right to reach MPP. Conversely, if an increase in voltage leads to a decrease in power, this means the operating point of the PV module is on the right of the MPP and hence further perturbation towards the left is required to reach MPP. The behavior of solar panel indicating MPP and operating principle is shown in Fig-4 which indicates that the resulting change of PV power is observed as follows: When the PV module operating point is on the left side of the curve ($\Delta P/\Delta V$ is positive), which means the PV module output power increases, the perturbation of the PV module voltage should be increased towards the MPP. If the operating point of the module was on the right side of the curve ($\Delta P/\Delta V$ is negative), then the perturbation of the PV module voltage should be decreased towards the MPP. The flowchart for implementation of the P and O algorithm first measures the practical voltage and current from PV array. After that, the product of voltage and current gives the actual power of PV module. Then, it will check the condition whether $\Delta P = 0$ or not. If this condition is satisfied, then operating point is at the MPP. If it is not satisfying, then it will check another condition that $\Delta P > 0$. If this condition is satisfied, then it will check that $\Delta V > 0$. If it is satisfied, then it indicates that operating point is at the left side of the MPP. If $\Delta V > 0$ condition is not satisfied, then it indicates that operating point is at the right side of the MPP. This process is continuously repeated until it reaches the MPP.

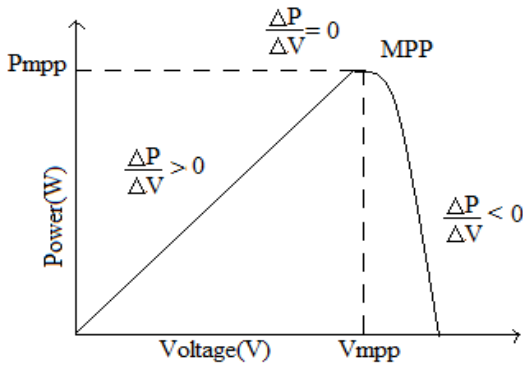


Fig -4: P vs V characteristics of the PV array

The power of PV array is,

$$P = V \times I \tag{35}$$

By differentiating it with respect to voltage, if

$$\frac{dP}{dV} > 0 \tag{36}$$

the operating point is on the left side of MPP.

$$\frac{dP}{dV} = 0 \tag{37}$$

the operating point is at MPP.

$$\frac{dP}{dV} < 0 \tag{38}$$

the operating point is on the right side of MPP.

On the right side of MPP, slope is negative, which suggests that $dP/dV < 0$ and on the left side slope is positive meaning $dP/dV > 0$. At MPP slope is zero means that $dP = 0$. The duty ratio of the boost converter is adjusted in accordance with the algorithm as shown in Fig -5.

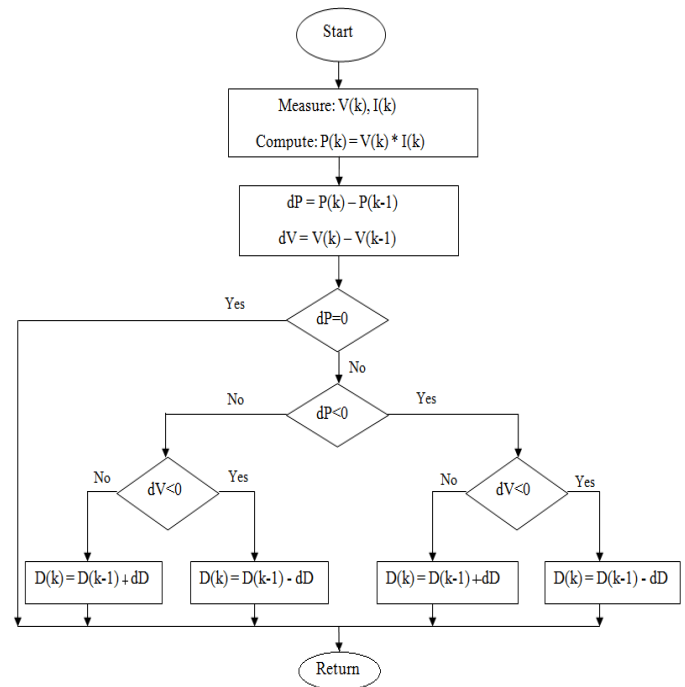


Fig-5: Flowchart for perturb and observe (P and O) algorithm for MPPT

3.2. Scalar (V/f) control of induction motor

The scalar control is most common and simplest control used in induction motor. The voltage has to be reduced for the operation at low speed. The frequency control along with voltage magnitude control is also required for constant flux operation. The voltage should be proportional to the frequency such that flux magnitude is maintained constant as $\psi_s = \frac{V}{\omega}$. An IM is usually fed from a three phase PWM VSI. Only an input parameter is the reference speed. Neglecting the small slip speed, the speed of the motor is approximately equal to the reference speed. The speed reference is integrated to generate the θ which is used to obtain three sinusoidal voltage references, which are compared with high frequency triangular wave to generate the switching pulses for VSI. The speed reference is estimated from the control scheme.

$$\theta = \int \omega^* dt \tag{39}$$

The 3 reference voltages are,

$$V_a^* = m \times \sin(\theta) \tag{40}$$

$$V_b^* = m \times \sin(\theta - 120^\circ) \tag{41}$$

$$V_c^* = m \times \sin(\theta - 240^\circ) \tag{42}$$

where, $m = K_f \omega^*$, m is the modulation index.

4. RESULTS AND DISCUSSION

The performance of a PV fed water pumping system is evaluated using the simulation software. The existing and proposed system is designed, modelled and simulated in the MATLAB/Simulink software. The change in the solar radiation is also simulated in order to determine the performance of the system under dynamic conditions.

4.1. At an irradiance of 1000 W/m²

For the proposed system, when the irradiance is 1000W/m² the output voltage across the PV array is 100V is shown in Fig -6 and the power of PV is 500W. It is shown in Fig -7. The ripples shown in output voltage of PV can be reduced by the filter capacitor C_f. It is shown in Fig -8. The Fig -9 shows that the voltage across the DC bus is maintained at 653V due to the action of PI controller.

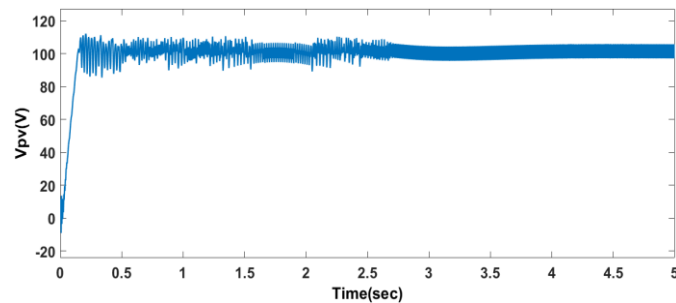


Fig -6: Waveform of output voltage of PV

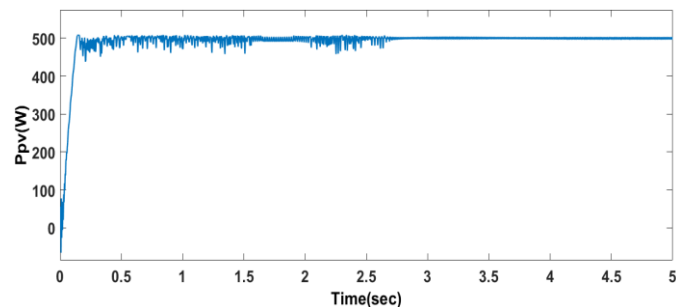


Fig -7: Waveform of output power of PV

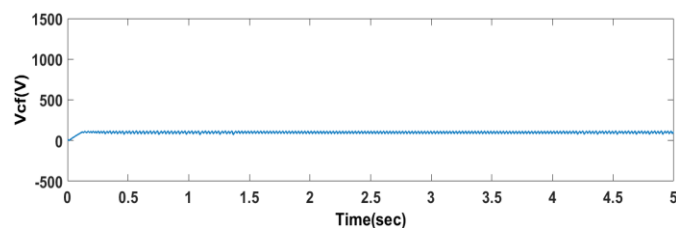


Fig -8: Waveform of voltage of capacitor C_f

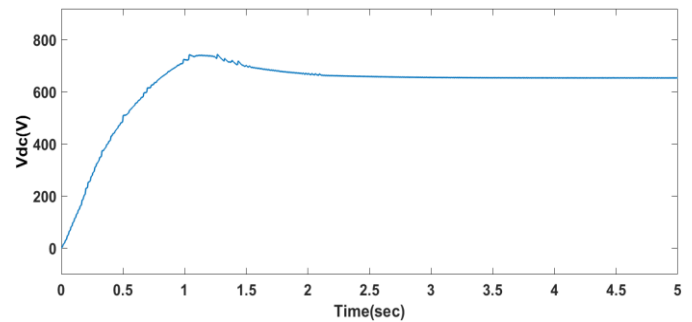


Fig -9: Waveform of voltage of DC bus

The Fig -10 shows the speed of induction motor. Here the speed of the induction motor is 1400 rpm. The Fig -11 shows the torque of induction motor. The induction motor torque is 2.5Nm.

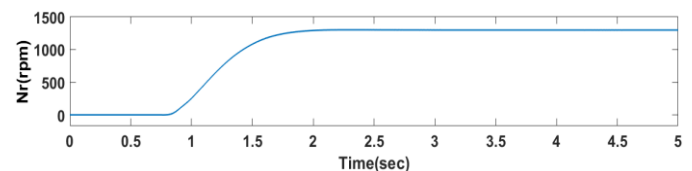


Fig -10: Waveform of speed of motor

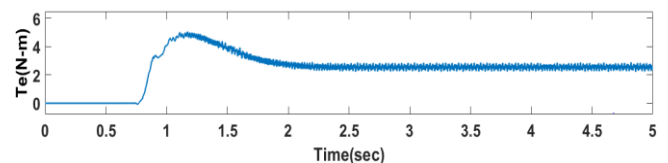


Fig -11: Waveform of motor torque

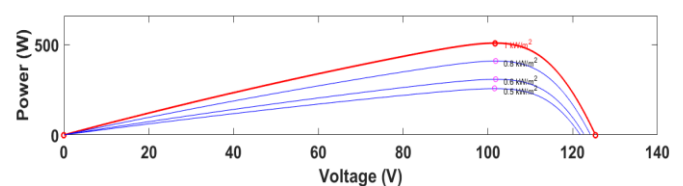


Fig -12: Waveform of MPP of P vs V for MPPT by P and O method

The Fig -12 shows the waveform of maximum power point of P vs V for MPPT by P and O method. Here the voltage at maximum power point is 101V. The red line shows when the irradiance is 1000W/m² and the blue line shows when the irradiance is reduced to 800W/m², 600W/m² and 500W/m². This shows that the V_{mpp} is maintained at constant value at these irradiances. But the power at the maximum power point changes. The Fig -13 shows the phase voltages of inverter. The phase voltages of V_{ab}, V_{bc} and V_{ac} are 653V. The Fig -14 shows the waveform of inverter phase current i_a. Here it shows

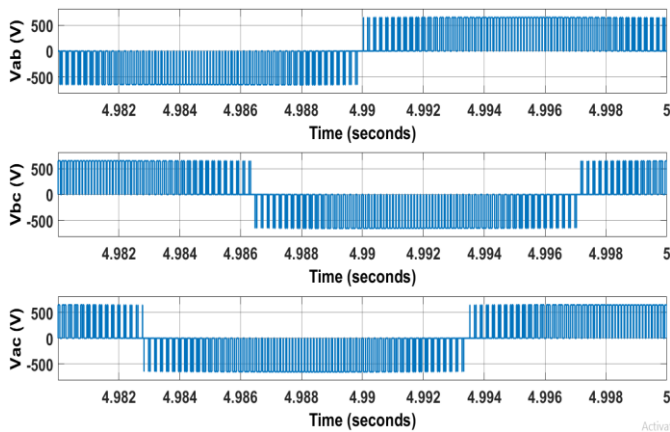


Fig -13: Waveform of phase voltages of inverter V_{ab} , V_{bc} , V_{ac}

some harmonic distortions in the waveform. The Fig -15 and Fig -16 shows the waveform of inverter phase current i_b and i_c . Here this shows that there are some distortions in the waveform. The Fig -17 shows the THD of inverter phase current i_a . Its THD is reduced to 3.91%. The Fig -18 shows the THD of phase current i_b . Its THD is reduced to 3.98%. The Fig -19 shows the THD of inverter phase current i_c . Its THD is reduced to 4.42%.

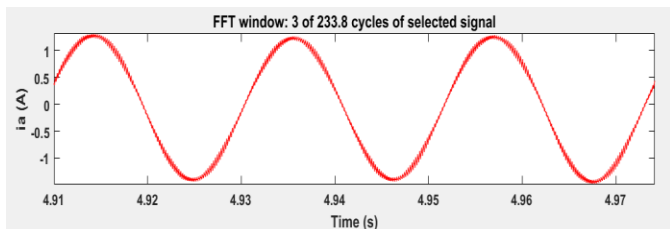


Fig -14: Waveform of inverter phase current i_a

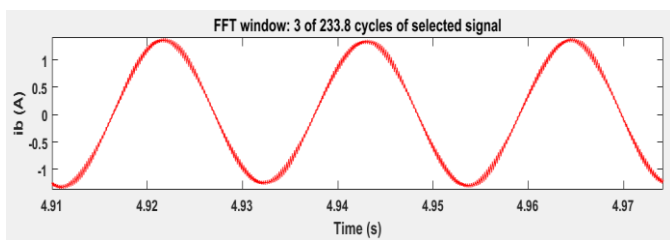


Fig -15: Waveform of inverter phase current i_b

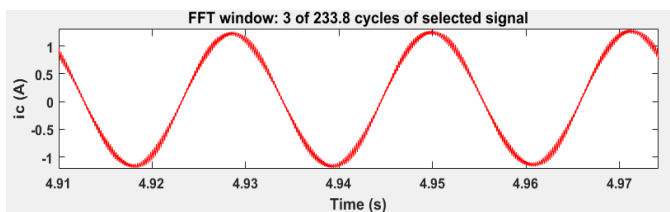


Fig -16: Waveform of inverter phase current i_c

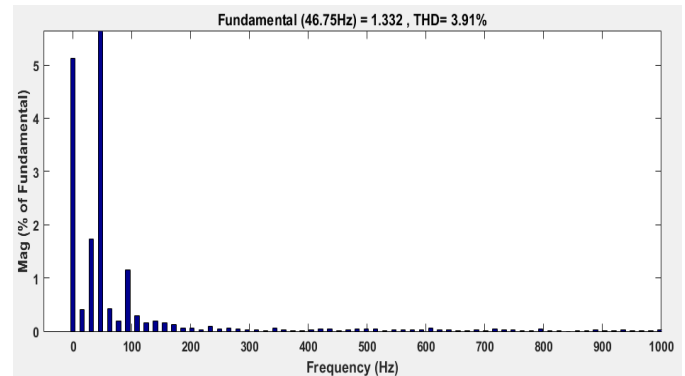


Fig -17: Waveform of THD of i_a

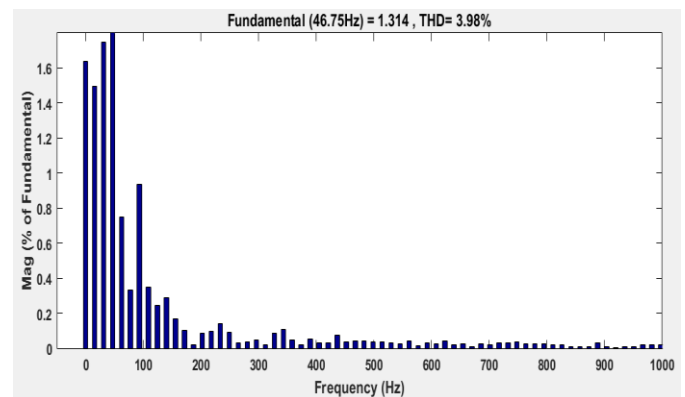


Fig -18: Waveform of THD of i_b

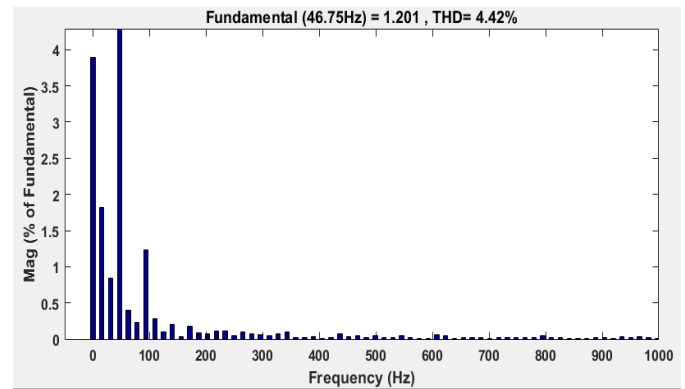


Fig -19: Waveform of THD of i_c

4.2. At an irradiance of 500 W/m²

For the proposed system, when the irradiance is reduced to 500W/m² the output voltage across the PV array is maintained at 100V is shown in Fig -20 and the power of PV is reduced to 250W. It is shown in Fig -21. The Fig -22 shows that the voltage across the DC bus is maintained at 653V due to the action of PI controller. So in varying solar radiations the DC bus voltage can be maintained constant. The Fig -23 shows the torque of induction motor. The induction motor torque is reduced to 1.44Nm.

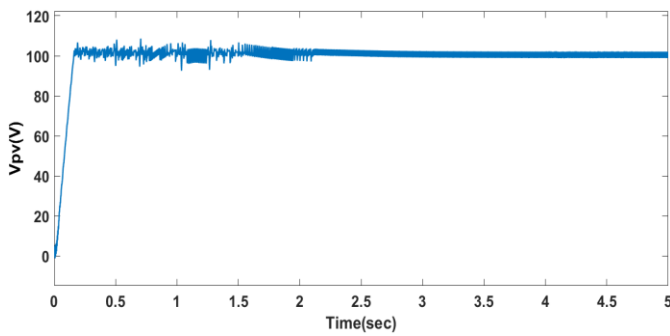


Fig -20: Waveform of output voltage of PV

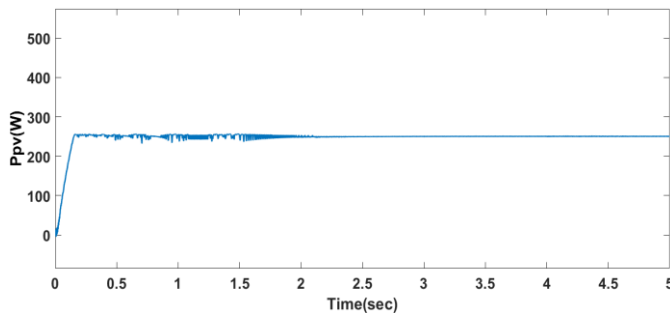


Fig -21: Waveform of output power of PV

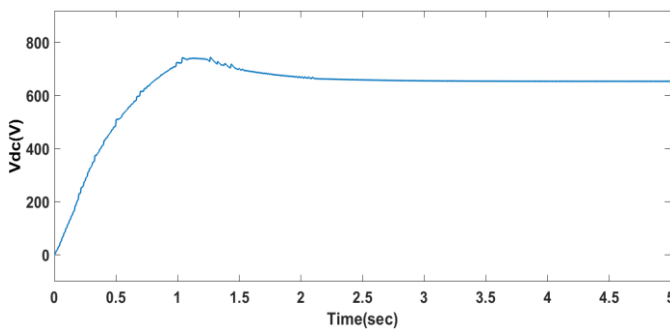


Fig -22: Waveform of voltage of DC bus

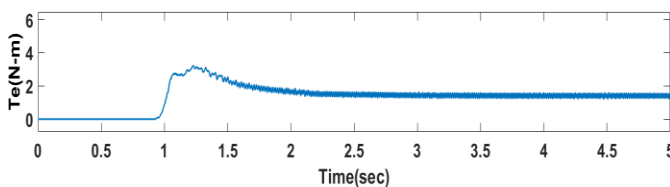


Fig -23: Waveform of torque of induction motor

5. COMPARISON BETWEEN EXISTING AND PROPOSED SYSTEM

The Table -2 shows when both system has solar irradiance of 1000W/m². By keeping the dc bus voltage constant at 653V for both the systems, the output voltage of PV has reduced by using a high gain converter. Thus the voltage and power of PV has reduced to 100V and 500W.

The existing and proposed system uses a 0.5HP induction motor. So by keeping the dc bus voltage and load constant, the number of solar modules are reduced so that the output voltage of PV can be reduced. Hence the number of solar modules used for existing system is 12 and the proposed system requires only 4 modules. So the size and cost of the system reduces. Then the THD of the inverter current i_a for the existing system is 15.19% it is reduced to 3.91% in the proposed system.

Table -2: Existing and proposed system parameters and values

Parameters	Existing system[1]	Proposed system
Irradiance	1000W/m ²	1000W/m ²
V _{PV}	372.9V	100V
P _{PV}	2.4KW	500W
V _{dc}	653V	653V
Speed	1400rpm	1400rpm
Torque	2.5Nm	2.5Nm
Induction motor	0.5HP	0.5HP
No: of modules	12	4
THD of i_a	15.19%	3.91%

The Table -3 shows the comparison between the existing and proposed system at different solar radiations. Here when solar radiation is reduced from 1000W/m² to 500W/m², the voltage of dc bus is maintained at constant for existing and proposed system. For proposed system by keeping the dc bus voltage and load constant, output voltage of PV is reduced by using a high gain converter. But the existing system uses a low gain boost converter so its output voltage of PV is more. The output voltage of PV is maintained constant for existing system at both irradiances and the proposed system at both irradiances due to the MPPT method. But the current and power of PV are reduced. The speed and torque are also reduced.

Table -3: Existing and proposed system parameters and values at varying solar radiations

Parameters	Existing system[1]		Proposed system	
	1000W/m ²	500W/m ²	1000W/m ²	500W/m ²
Irradiance	1000W/m ²	500W/m ²	1000W/m ²	500W/m ²
V _{PV}	372.9V	372.9V	100V	100V
I _{PV}	6.63A	3.31A	5A	2.5A
P _{PV}	2.4KW	1.2KW	500W	250W
V _{dc}	653V	653V	653V	653V

N_r	1400rpm	904rpm	1400rpm	904rpm
T	2.5Nm	1.4Nm	2.5Nm	1.44Nm

6. CONCLUSION

The water pumping system with a high gain converter has been proposed. Here by using this converter the number of solar modules are reduced so that the output voltage of PV can also be reduced. Thus the size and cost of the system are reduced. The number of computational steps for the MPPT algorithm has reduced due to the P and O method. The system tracks the MPP with acceptable tolerance even at varying radiation. The THD of the inverter current has also been reduced. So this proposed system can maintain the DC link voltage to a constant voltage to a constant by the action of PI controller in varying radiations. Its feasibility of operation has been verified through simulation results. The performance conditions in varying solar radiations have been verified.

REFERENCES

[1] Bhim Singh, Utkarsh Sharma and Shailendra Kumar, "Standalone photovoltaic water pumping system using induction motor drive with reduced sensors," IEEE Transactions on Industry Applications, vol. 3, no.2, pp.2825-2833, August 2018.

[2] E. Muljadi, "PV water pumping with a peak-power tracker using a simple six-step square-wave inverter," IEEE Transactions on Industrial Applications, vol. 33, no. 3, pp. 714-721, May-June 1997.

[3] U. Sharma, S. Kumar and B. Singh, "Solar array fed water pumping system using induction motor drive," 1st IEEE International Conference on Power Electronics, Intelligent Control and Energy Systems (ICPEICES), Delhi, March 2016.

[4] R. Kumar and B. Singh, "BLDC Motor-Driven Solar PV Array-Fed Water Pumping System Employing Zeta Converter," IEEE Transactions on Industrial Applications, vol. 52, no. 3, pp. 2315-2322, May-June 2016.

[5] J. Caracas, G. Farias, L.Teixeira and L. Ribeiro, "Implementation of a High-Efficiency, High-Lifetime, and Low-Cost Converter for an Autonomous Photovoltaic Water Pumping System," IEEE Transactions on Industrial Applications, vol. 50, no. 1, pp. 631-641, January-February 2014.

[6] Trishan Eshram and Patrick L. Chapman, "Comparison of photovoltaic array maximum power point tracking techniques," IEEE Transactions on Energy Conversion, vol. 22, no.2, pp. 439, June 2007.

[7] Subudhi and R. Pradhan, "A comparative study on maximum power point tracking techniques for photovoltaic power systems," IEEE Transactions on

Sustainable Energy, vol. 4, no. 1, pp. 89-98, January 2013.

[8] A. Garrigos, J. Blanes, J. Carrasco, and J. Ejea, "Real time estimation of photovoltaic modules characteristics and its application to maximum power point operation," IEEE Transactions on Renewable Energy, vol. 32, pp. 1059-1076, August 2007.

[9] B. Singh, S. Kumar and C. Jain, "Damped-SOGI-Based Control Algorithm for Solar PV Power Generating System," IEEE Transactions on Industrial Applications, vol. 53, no. 3, pp. 1780-1788, May-June 2017.

[10] X. D. Sun, K. H. Koh, B. G. Yu and M. Matsui, "Fuzzy-Logic Based V/f Control of an Induction Motor for a DC Grid Power- Levelling System Using Flywheel Energy Storage Equipment," IEEE Transactions on Industrial Electronics, vol. 56, no. 8, pp. 3161-3168, August 2009.

[11] S. R. Bhat, A. Pittet and B. S. Sonde, "Performance Optimization of Induction Motor-Pump System Using Photovoltaic Energy Source," IEEE Transactions on Industrial Applications, vol. IA-23, no. 6, pp. 995-1000, November 1987.

[12] Y. Yao, P. Bustamante and R. Ramshaw, "Improvement of induction motor drive systems supplied by photovoltaic arrays with frequency control," IEEE Transactions on Energy Conversion, vol. 9, no. 2, pp. 256-262, June 1994.

[13] U. Sharma, B. Singh and S. Kumar, "Intelligent grid interfaced solar water pumping system," IET Renewable Power Generation, vol. 11, no. 5, pp. 614-624, March 2017.

[14] Faramarz Karbakhsh, Mehdi Amiri and Hossein Abootorabi Zarchi, "Two-switch flyback inverter employing a pumps," IET Renewable Power Generation, vol. 11, no. 5 current sensorless MPPT and scalar control for low cost solar powered, June 2017.

[15] S. Jain, R. Karampuri and V. Somasekhar, "An Integrated Control Algorithm for a Single-Stage PV Pumping System Using an Open-End Winding Induction Motor," IEEE Transactions on Industrial Electronics, vol. 63, no. 2, pp. 956-965, February 2016.

[16] Hussein M Waly, Dina S M Osheba, Haitham Z Azazi and Awad E El-Sabbe "Induction Motor Drive for PV Water-Pumping System with High Gain Non Isolated DC-DC Converter," IEEE Transactions on Power Electronics and Renewable Energy, vol. 4, no. 9, pp. 4809-4818, Sept. 2019.

[17] Rajan V Vamja and Mahmadasraf A Mulla, "Solar PV Fed Induction Motor Driven Water Pumping System utilizing Quadratic Boost Converter," IEEE Transactions on Renewable Energy, vol. 32, pp. 1045-1053, March 2018.

[18] I Daut, N Gomesh and Y M Irawan,, "Parameter Determination of 0.5hp Induction Motor Based on Load Factor Test-a Case Study," International Conference on Electrical, Control and Computer Engineering, vol. 63, no. 2, pp. 956-965, June 2011.

- [19] A. Achour, D. Rekioua, A. Mohammedi, Z. Mokrani, T. Rekioua, S. Bacha, "Application of Direct Torque Control to a Photovoltaic Pumping System with Sliding-mode Control Optimization," IEEE Transactions on Electric Power Components and Systems, vol. 44, no. 2, January 2016.
- [20] C. Slabbert and M. Malengret, "Grid connected/solar water pump for rural areas," Proceedings of ISIE '98. IEEE International Symposium on Industrial Electronics, Pretoria, pp. 31-34 vol.1, August 1998.